ON THE THERMOMECHANICAL COUPLING IN SHAPE MEMORY ALLOYS

Paulo Cesar da Camara Monteiro Jr., camara@lts.coppe.ufrj.br
Universidade Federal do Rio de Janeiro, COPPE - Departamento de Engenharia Oceânica
Marcelo Amorim Savi, savi@mecanica.ufrj.br
Universidade Federal do Rio de Janeiro, COPPE - Departamento de Engenharia Mecânica
Theodoro Antoun Netto, tanetto@lts.coppe.ufrj.br
Universidade Federal do Rio de Janeiro, COPPE - Departamento de Engenharia Oceânica
Pedro M.C.L. Pacheco, calas@cefet-rj.br
CEFET/RJ - Departamento de Engenharia Mecânica

Abstract. *Constitutive models are interested in phenomenological features and although there is a great number of constitutive models to describe the thermomechanical behavior of shape memory alloys (SMAs), this description stills the objective of many research efforts. Usually, these models analyze the thermal and the mechanical behaviors in an uncoupled way. This contribution analyzes the SMA behavior considering the thermomechanical coupling. The constitutive model is developed in the framework of continuum mechanics. An experimental verification comparing experimental results with those obtained by numerical simulations of the proposed model is of concern. Numerical simulations are carried out showing the capability of the model to describe different aspects of SMA thermomechanical behavior, especially those related to the thermomechanical coupling. Moreover, it is noticeable that the uncoupled model (neglecting energy equation thermomechanical terms) is rate-dependent being capable to capture some important features of SMA behavior.*

Keywords: *Shape memory alloys, constitutive model, thermomechanical coupling, rate-dependence*

1. INTRODUCTION

Shape memory alloys (SMAs) present complex thermomechanical behaviors related to different physical processes, such as pseudoelasticity, shape memory effect, which may be one-way (SME) or two-way (TWSME), and phase transformation due to temperature variation. Besides, there are more complicated phenomena that have significant influence over its overall thermomechanical behavior - for instance: plastic behavior, tension-compression asymmetry, plastic-phase transformation coupling, transformation induced plasticity, thermomechanical coupling, among others.

The hysteretic response of SMAs is one of their essential characteristics being related to the martensitic phase transformation. The hysteresis loop is mainly caused by frictional effects associated with the movement of austenite-martensite interfaces and martensite-martensite interfaces with different crystallographic orientations. Basically, the hysteresis loop may be observed either in stress-strain curves or in strain-temperature curves. In brief, it is possible to say that the major (or external) hysteresis loop can be defined as the envelope of all minor (or internal) hysteresis loops, usually denoted as subloops (Bo & Lagoudas, 1999).

The thermomechanical behavior of SMAs has been described by different mathematical models that capture the main behaviors of these alloys. The macroscopic approach is interested on SMAs' phenomenological features. (Paiva & Savi, 2006) present an overview of the main macroscopic models discussed in literature. A model that is capable to describe the main thermomechanical features of SMAs in a flexible way is presented in a series of references (Savi et al., 2002; Baêta-Neves et al., 2004; Paiva et al., 2005; Savi & Paiva, 2005). Basically, this one-dimensional constitutive model considers different material properties and four macroscopic phases for the description of the SMA behavior. The model also considers the plastic strains and plastic-phase transformation coupling, which turns possible the two-way shape memory effect description. Moreover, tensile-compressive asymmetry is taken into account.

As it is well-known, SMA devices present a rate-dependence characteristic that means that the thermomechanical response depends on loading rate (Shaw & Kyriades, 1995). Some authors point that this behavior results from the thermomechanical coupling effect associated with the latent heat due phase transformation (Auricchio et al., 2007; Shaw & Kyriades, 1995). The thermomechanical coupling is related to an endothermic process that occurs during the phase transformation from austenite to martensite and also an exothermic process associated with the reverse transformation. Therefore, although martensitic transformation is non-diffusive, the phase transformation critical stresses are temperature dependent and, since heat transfer process (conduction and convection) is time dependent, it affects the thermomechanical behavior of SMAs. Therefore, it is of great interest to propose rate-dependent models that can capture this general characteristics of SMAs.

2. Mathematical Modeling

The thermomechanical coupling may be proper modeled in the framework of continuum mechanics. Therefore, in order to obtain a better comprehension of the formulation, it is presented a brief review concerning first and second principle of thermodynamics. The local form of the Clausius-Duhem inequality may be written as follows:

$$\sigma\dot{\varepsilon} - \rho\left(\dot{\psi} - s\dot{T}\right) - \frac{q}{T}\frac{\partial T}{\partial x} \geq 0, \tag{1}$$

where ρ is the specific mass, ψ the Helmholtz free energy, s specific entropy, T temperature, σ the uniaxial stress, ε total strain and q is the heat flux. As a first hypothesis concerning the constitutive modeling, it is assumed that the Helmholtz free energy is a function of a finite set of variables:

$$\psi = \psi\left(\varepsilon, \varepsilon^i, T, V\right), \tag{2}$$

where ε^i is the inelastic strain and V represent a set of internal variables of the problem. Since

$$\dot{\psi} = \frac{\partial\psi}{\partial\varepsilon}\dot{\varepsilon} + \frac{\partial\psi}{\partial\varepsilon^i}\dot{\varepsilon}^i + \frac{\partial\psi}{\partial T}\dot{T} + \frac{\partial\psi}{\partial V}\dot{V}. \tag{3}$$

the Clausius-Duhem inequality may be rewritten as follows:

$$\left(\sigma - \rho\frac{\partial\psi}{\partial\varepsilon}\right)\dot{\varepsilon} - \rho\frac{\partial\psi}{\partial\varepsilon^i}\dot{\varepsilon}^i - \rho\frac{\partial\psi}{\partial V}\dot{V} - \rho\left(s + \frac{\partial\psi}{\partial T}\right)\dot{T} - \frac{q}{T}\frac{\partial T}{\partial x} \geq 0. \tag{4}$$

Motivated by the Clausius-Duhem inequality, it is convenient to establish the following definitions of thermodynamics force:

$$\sigma = -\rho\frac{\partial\psi}{\partial\varepsilon}; \quad \sigma^i = \rho\frac{\partial\psi}{\partial\varepsilon^i}; \quad A = \rho\frac{\partial\psi}{\partial V} \tag{5}$$

$$s = -\frac{\partial\psi}{\partial T}; \quad g = \frac{\partial T}{\partial x}. \tag{6}$$

In order to describe irreversible processes, it is interesting to define a pseudo-potential of dissipation, φ, that can establish the variable evolution laws. This dissipative potential may be split into intrinsic (or mechanical) and thermal dissipation. By assuming that it is a positive, convex function that vanishes at the origin, the Clausius-Duhen inequality is automatically satisfied defining the thermodynamic fluxes as follows:

$$\sigma^i = \frac{\partial\varphi}{\partial\dot{\varepsilon}^i}, \qquad A = \frac{\partial\varphi}{\partial\dot{V}} \qquad g = -\frac{\partial\varphi}{\partial\left(q/T\right)}\ . \tag{7}$$

Alternatively, these thermodynamics fluxes may be obtained from the dual of the potential of dissipation, φ^* allowing the definitions:

$$\dot{\varepsilon}^i = \frac{\partial\varphi^*}{\partial\sigma^i} \qquad \dot{V} = \frac{\partial\varphi^*}{\partial A} \qquad q/T = -\frac{\partial\varphi^*}{\partial g}\ . \tag{8}$$

At this point, it is necessary to establish the energy conservation equation given by the first principle of thermodynamics:

$$\rho\dot{\psi} = \sigma\dot{\varepsilon} - \frac{\partial q}{\partial x} - \rho T\dot{s} - \rho\dot{T}s. \tag{9}$$

Since we are interested in a single point description, it is neglected variable spatial variations and also it is assumed a convection boudary condition. Therefore, the first principle of thermodynamics has the following form:

$$\dot{T} = \frac{1}{\rho c}\left[hA(T - T_\infty) + \sigma^i\dot{\varepsilon}^i - A\dot{V} + T\left(\frac{\partial\sigma}{\partial T}\dot{\varepsilon} + \frac{\partial A}{\partial T}\dot{V}\right)\right], \tag{10}$$

where c is the specific heat.

2.1 Constitutive Model

There are different ways to describe the thermomechanical behavior of SMAs (Paiva & Savi, 2006). Here, a constitutive model that is built upon the Fremond's model and previously presented in different references (Savi et al., 2002; Baêta-Neves et al., 2004; Paiva et al., 2005; Savi & Paiva, 2005) is employed. This model considers different material properties and four macroscopic phases for the description of the SMA behavior. The tension-compression asymmetry, the plastic strain and the plastic-phase transformation coupling are incorporated in the original model. It should be highlighted that this model is rate-dependent, being capable to capture some important features of SMA behavior.

Here, the thermomechanical coupling is of concern. The continuum mechanics framework, briefly presented in the previous section, is employed to obtain the general constitutive equations. The model presentation starts assuming Helmholtz free energy of each isolated phase. With this aim, consider four macroscopic phases: austenite $\mathbf{A}$, twinned martensite $\mathbf{M}$, positive detwinned martensite $\mathbf{M}^+$ and negative detwinned martensite $\mathbf{M}^-$. Here, besides elastic strain ε^e, temperature, T, it is assumed variables related to isotropic and kinematics hardening, respectively, γ and μ. These functions consider the following material parameters, where it is assumed a subscript $\mathbf{A}$ for austenitic phase and $\mathbf{M}$ for martensitic phase: E is the elastic modulus, Ω is related to thermal expansion coefficient, K is the isotropic hardening parameter and H is the kinematics hardening parameter. T_0 is a reference temperature, α is related to the hysteresis loop vertical size. Finally, Λ is a temperature dependent function.

$$M^+ : \rho\psi_1\left(\varepsilon_e, T, \gamma, \mu\right) = \frac{1}{2}E_M{\varepsilon_e}^2 - \alpha^T\varepsilon_e - \Gamma_1 - \Omega_M\left(T - T_0\right)\varepsilon_e + \frac{1}{2}K_M\gamma^2 + \frac{1}{2H_M}\mu^2; \tag{11}$$

$$M^- : \rho\psi_2\left(\varepsilon_e, T, \gamma, \mu\right) = \frac{1}{2}E_M{\varepsilon_e}^2 + \alpha^C\varepsilon_e - \Gamma_2 - \Omega_M\left(T - T_0\right)\varepsilon_e + \frac{1}{2}K_M\gamma^2 + \frac{1}{2H_M}\mu^2; \tag{12}$$

$$A : \rho\psi_3\left(\varepsilon_e, T, \gamma, \mu\right) = \frac{1}{2}E_A{\varepsilon_e}^2 - \Gamma_3 - \Omega_A\left(T - T_0\right)\varepsilon_e + \frac{1}{2}K_A\gamma^2 + \frac{1}{2H_A}\mu^2; \tag{13}$$

$$M : \rho\psi_4\left(\varepsilon_e, T, \gamma, \mu\right) = \frac{1}{2}E_M{\varepsilon_e}^2 - \Gamma_4 - \Omega_M\left(T - T_0\right)\varepsilon_e + \frac{1}{2}K_M\gamma^2 + \frac{1}{2H_M}\mu^2, \tag{14}$$

Now, it is possible to define the mixture free specific energy, defining volumetric fractions for each phase: β_1 and β_2 are respectively, the positive $\mathbf{M}^+$ and negative $\mathbf{M}^-$ detwinned martensites, β_3 is associated with austenitic phase $\mathbf{A}$, and β_4 is related to twinned martensite $\mathbf{M}$. Since $\beta_4 = 1 - \beta_1 - \beta_2 - \beta_3$, it is possible to write an equation with only three volumetric fractions as follows

$$\tilde{\psi}\left(\varepsilon_e, T, \gamma, \mu\right) = \sum_{k=1}^{3}\beta_n\psi_k + \tilde{J}_\Pi\left(\beta_1, \beta_2, \beta_3\right) + \tilde{J}_\Xi\left(\dot{\beta}_1, \dot{\beta}_2, \dot{\beta}_3\right), \tag{15}$$

By assuming a additive decomposition $\varepsilon_e = \varepsilon - \varepsilon_p - \alpha_h^T\beta_1 + \alpha_h^C\beta_2$ where α_T is related to the horizontal hysteresis loop size, the free specific energy can be written in an expanded form:

$$\begin{aligned}\tilde{\psi}\left(\varepsilon_e, T, \gamma, \mu\right) \quad = \quad & -\left[\alpha^T\left(\varepsilon - \varepsilon_p - \alpha_h^T\beta_1 + \alpha_h^C\beta_2\right) - \Lambda_1\right]\beta_1 + \\ & +\left[\alpha^C\left(\varepsilon - \varepsilon_p - \alpha_h^T\beta_1 + \alpha_h^C\beta_2\right) + \Lambda_2\right]\beta_2 + \\ & +\frac{1}{2}E\left(\varepsilon - \varepsilon_p - \alpha_h^T\beta_1 + \alpha_h^C\beta_2\right)^2 + \\ & -\Omega\left(T - T_0\right)\left(\varepsilon - \varepsilon_p - \alpha_h^T\beta_1 + \alpha_h^C\beta_2\right) + \frac{1}{2}K\gamma^2 + \frac{1}{2H}\mu^2 + \\ & +\Lambda_3\beta_3 + \Gamma_4 + \tilde{J}_\Pi\left(\beta_1, \beta_2, \beta_3\right) + \tilde{J}_\Xi\left(\dot{\beta}_1, \dot{\beta}_2, \dot{\beta}_3\right),\end{aligned} \tag{16}$$

where $\tilde{J}_\Pi$ is the indicator function related to the convex set Π, associated with the phase coexistence, that has the following form:

$$\Pi = \{\beta_k \in \Re \,|\, 0 \leq \beta_k \leq 1, k = 1 \ldots 3. \tag{17}$$

Moreover $\tilde{J}_{\Xi}$ is the indicator function of the convex set Ξ used to describe subloops due to incomplete phase transformation and also to avoid transformations of the type $\mathbf{M} \rightarrow \mathbf{M}^{+}$ and $\mathbf{M} \rightarrow \mathbf{M}^{-}$.

$\sigma \neq 0, k = 1 \ldots 3$

$$\Xi = \left\{ \dot{\beta}_k \in \Re \;\middle|\; \begin{array}{lll} \dot{\varepsilon}\dot{\beta}_1 \geq 0 & \text{and} & \dot{\varepsilon}\dot{\beta}_3 \leq 0 \quad \text{if} \quad \varepsilon_0 > 0 \\ \dot{\varepsilon}\dot{\beta}_2 \leq 0 & \text{and} & \dot{\varepsilon}\dot{\beta}_3 \geq 0 \quad \text{if} \quad \varepsilon_0 < 0 \end{array} \right. \tag{18}$$

where $\varepsilon_0 = \varepsilon - \Omega / E\,(T - T_0)$.

$\sigma = 0, k = 1 \ldots 3$

$$\Xi = \left\{ \dot{\beta}_k \in \Re \;\middle|\; \begin{array}{ll} \dot{T}\dot{\beta}_1 \left| \begin{array}{ll} < 0, & \text{if} \quad \dot{T} > 0,\ \sigma < \sigma_M^{Crit} \quad \text{and} \quad \beta_1^S \neq 0 \\ = 0, & \text{otherwise} \end{array} \right. \\ \dot{T}\dot{\beta}_2 \left| \begin{array}{ll} < 0, & \text{if} \quad \dot{T} > 0,\ \sigma < \sigma_M^{Crit} \quad \text{and} \quad \beta_2^S \neq 0 \\ = 0, & \text{otherwise} \end{array} \right. \\ \dot{T}\dot{\beta}_3 \geq 0 \end{array} \right. \tag{19}$$

In the Ξ set, β_1^S e β_2^S represent the volumetric fraction of detwinned martensite in the beginning of phase transformation, σ_M^{Crit} is the critical stress.

It should be noticed that the mixture material parameters has the following form:

$$E = E_M + (E_A - E_M)\,\beta_3\,, \quad \Omega = \Omega_M + (\Omega_A - \Omega_M)\,\beta_3; \tag{20}$$

$$K = K_M + (K_A - K_M)\,\beta_3\,, \quad \frac{1}{H} = \frac{1}{H_M} + \left(\frac{1}{H_A} + \frac{1}{H_M} \right) \beta_3; \tag{21}$$

Moreover, temperature dependent functions are assumed to be given by:

$$\Lambda_1 = \Gamma_4 - \Gamma_1 = -L_0^T + \frac{L^T}{T_M}\,(T - T_M)\,; \tag{22}$$

$$\Lambda_2 = \Gamma_4 - \Gamma_2 = -L_0^C + \frac{L^C}{T_M}\,(T - T_M)\,; \tag{23}$$

$$\Lambda_3 = \Gamma_4 - \Gamma_3 = -L_0^A + \frac{L^A}{T_M}\,(T - T_M)\,; \tag{24}$$

At this point, it is employed the definitions discussed in the previous sections. Therefore, the thermodynamics forces are obtained:

$$\sigma = \rho \frac{\partial \tilde{\psi}}{\partial \varepsilon} = E\left(\varepsilon - \varepsilon^p - \alpha_h^T \beta_1 + \alpha_h^C \beta_2\right) - \alpha^T \beta_1 + \alpha^C \beta_2 - \Omega\,(T - T_0)\,; \tag{25}$$

$$\begin{aligned} B_1 \in -\rho \partial_1 \tilde{\psi} \quad = \quad & \alpha^T\,(\varepsilon - \varepsilon^p) + \Lambda_1 - \left[2\alpha_h^T \alpha^T + E\left(\alpha_h^T\right)^2 \right] \beta_1 + \\ & + \left(\alpha_h^C \alpha^T + \alpha_h^T \alpha^C + E \alpha_h^T \alpha_h^C \right) \beta_2 + \\ & + \alpha_h^T \left[E\,(\varepsilon - \varepsilon^p) - \Omega\,(T - T_0) \right] - \partial_1 J_{\Pi}; \end{aligned} \tag{26}$$

$$\begin{aligned} B_2 \in -\rho \partial_2 \tilde{\psi} \quad = \quad & -\alpha^C\,(\varepsilon - \varepsilon^p) + \Lambda_2 + \left[2\alpha_h^C \alpha^C + E\left(\alpha_h^C\right)^2 \right] \beta_2 + \\ & - \left(\alpha_h^T \alpha^C + \alpha_h^C \alpha^T + E \alpha_h^C \alpha_h^T \right) \beta_1 + \\ & + \alpha_h^C \left[E\,(\varepsilon - \varepsilon^p) - \Omega\,(T - T_0) \right] - \partial_2 J_{\Pi}; \end{aligned} \tag{27}$$

$$\begin{aligned} B_3 \in -\rho\partial_3\tilde{\psi} &= \frac{1}{2}\left(E_A - E_M\right)\left(\varepsilon - \varepsilon^p - \alpha_h^T\beta_1 + \alpha_h^C\beta_2\right)^2 + \Lambda_3 + \\ &+ \left(\Omega_A - \Omega_M\right)\left(T - T_0\right)\left(\varepsilon - \varepsilon^p - \alpha_h^T\beta_1 + \alpha_h^C\beta_2\right) + \\ &- \frac{1}{2}\left(K_M - K_A\right)\gamma^2 + \left(\frac{1}{2H_M} - \frac{1}{2H_A}\right)\mu^2 - \partial_3 J_\Pi \end{aligned} \tag{28}$$

$$X = -\rho\frac{\partial\psi}{\partial\varepsilon^p} = E\left(\varepsilon - \varepsilon^p - \alpha_h^T\beta_1 + \alpha_h^C\beta_2\right) - \alpha^T\beta_1 + \alpha^C\beta_2 - \Omega\left(T - T_0\right) = \sigma \tag{29}$$

$$Y = -\rho\frac{\partial\tilde{\psi}}{\partial\gamma} = -K\gamma \tag{30}$$

$$Z = -\rho\frac{\partial\tilde{\psi}}{\partial\mu} = -\frac{1}{H}\mu \tag{31}$$

where ∂_1, ∂_2 e ∂_3 are sub-differentials of the indicator function J_Π with respect to β_1, β_2 e β_3 respectively (Rockafellar, 1970). In the same way, the dual of the dissipation potential is considered to be as follows:

$$\varphi* = \frac{1}{2\eta_1}\left(B_1 + \eta_{ci}Y + \eta_{ck}Z\right)^2 + \frac{1}{2\eta_2}\left(B_2 + \eta_{ci}Y + \eta_{ck}Z\right)^2 + \frac{1}{2\eta_3}\left(B_3 + \eta_{ci}Y + \eta_{ck}Z\right)^2 - \frac{q}{T}\frac{\partial T}{\partial x} + I_f \tag{32}$$

where I_f is the function associated to the yield surface:

$$f = \left|X + HY\right| - \left(\sigma_Y - Y\right), \tag{33}$$

and the thermodynamics fluxes are given by.

$$\dot{\beta}_1 \in \partial_{B_1}\varphi^* = \frac{1}{\eta_1}\left(B_1 - \eta_{ci}Y - \eta_{ck}Z\right) \tag{34}$$

$$\dot{\beta}_2 \in \partial_{B_2}\varphi^* = \frac{1}{\eta_2}\left(B_2 - \eta_{ci}Y - \eta_{ck}Z\right) \tag{35}$$

$$\dot{\beta}_3 \in \partial_{B_3}\varphi^* = \frac{1}{\eta_3}\left(B_3 + \eta_{ci}Y + \eta_{ck}Z\right) \tag{36}$$

$$\dot{\varepsilon}_p \in \partial_X\varphi^* = \lambda\frac{\left(X + HZ\right)}{\left|X + HZ\right|} \tag{37}$$

$$\dot{\gamma} \in \partial_Y\varphi^* = \lambda + \eta_{ci}\left(\dot{\beta}_1 + \dot{\beta}_2 - \dot{\beta}_3\right) \tag{38}$$

$$\dot{\mu} \in \partial_Z\varphi^* = \lambda H\frac{\left(X + HZ\right)}{\left|X + HZ\right|} + \eta_{ck}\left(\dot{\beta}_1 + \dot{\beta}_2 - \dot{\beta}_3\right), \tag{39}$$

Therefore, it is obtained a complete set of constitutive equations that completely describe the thermomechanical behavior of shape memory alloys:

$$\begin{aligned} \eta_1\dot{\beta}_1 &= \alpha^T\left(\varepsilon - \varepsilon^p\right) - \Lambda_1 - \left[2\alpha_h^T\alpha^T + E\left(\alpha_h^T\right)^2\right]\beta_1 + \\ &+ \left(\alpha_h^C\alpha^T + \alpha_h^T\alpha^C + E\alpha_h^T\alpha_h^C\right)\beta_2 + \\ &+ \alpha_h^T\left[E\left(\varepsilon - \varepsilon_p\right) - \Omega\left(T - T_0\right)\right] + \\ &+ \eta_{ci}K\gamma + \eta_{ck}\frac{1}{H}\mu - \frac{\partial J_\Pi}{\partial\beta_1} + \eta_T\frac{\partial J_\Xi}{\partial\beta_1}; \end{aligned} \tag{40}$$

$$\begin{aligned} \eta_2\dot{\beta}_2 &= -\alpha^C\left(\varepsilon - \varepsilon^p\right) - \Lambda_2 - \left(\alpha_h^T\alpha^C + \alpha_h^C\alpha^T + E\alpha_h^T\alpha_h^C\right)\beta_1 + \\ &+ \left[2\alpha_h^C\alpha^C + E\left(\alpha_h^C\right)^2\right]\beta_2 + \\ &+ \alpha_h^T\left[E\left(\varepsilon - \varepsilon_p\right) - \Omega\left(T - T_0\right)\right] + \\ &+ \eta_{ci}K\gamma + \eta_{ck}\frac{1}{H}\mu - \frac{\partial J_\Pi}{\partial\beta_2} + \eta_C\frac{\partial J_\Xi}{\partial\beta_2}; \end{aligned} \tag{41}$$

$$\begin{aligned}\eta_3\dot{\beta}_3 &= -\frac{1}{2}\left(E_A - E_M\right)\left(\varepsilon - \varepsilon^p - \alpha_h^T\beta_1 + \alpha_h^C\beta_2\right)^2 + \Lambda_3 + \\ &+ \left(\Omega_A - \Omega_M\right)\left(T - T_0\right)\left(\varepsilon - \varepsilon^p - \alpha_h^T\beta_1 + \alpha_h^C\beta_2\right) + \qquad (42)\\ &-\frac{1}{2}\left(K_M - K_A\right)\gamma^2 + \left(\frac{1}{2H_M} - \frac{1}{2H_A}\right)\mu^2 + \\ &+\eta_{ci}K\gamma + \eta_{ck}\frac{1}{H}\mu - \frac{\partial J_\Pi}{\partial\beta_3} + \eta_A\frac{\partial J_\Xi}{\partial\beta_3}; \qquad (43)\end{aligned}$$

$$\dot{\varepsilon}_p = \frac{\partial\varphi*}{\partial X} = \lambda\frac{(\sigma - \mu)}{|\sigma - \mu|} \qquad (44)$$

$$\dot{\gamma} = \frac{\partial\varphi*}{\partial Y} = |\dot{\varepsilon}_p| + \eta_{ci}\left(\dot{\beta}_1 + \dot{\beta}_2 - \dot{\beta}_3\right) \qquad (45)$$

$$\dot{\mu} = \frac{\partial\varphi*}{\partial Y} = H\,|\dot{\varepsilon}_p| + \eta_{ck}\left(\dot{\beta}_1 + \dot{\beta}_2 - \dot{\beta}_3\right), \qquad (46)$$

where η_1, η_2 and η_3 represent the internal dissipation related to phase transformation. The temperature variation is described by the following energy equation that incorporate thermomechanical coupling terms:

$$\begin{aligned}\rho c\dot{T} &= hA\left(T - T_\infty\right) + \sigma\dot{\varepsilon}^p - \left(B_1\dot{\beta}_1 + B_2\dot{\beta}_2 + B_3\dot{\beta}_3\right) - Y\dot{\gamma} - Z\dot{\mu} + \\ &+T\left[-\frac{\partial\sigma}{\partial T}\left(\dot{\varepsilon} - \dot{\varepsilon}^p\right) + \frac{\partial B_1}{\partial T}\dot{\beta}_1 + \frac{\partial B_2}{\partial T}\dot{\beta}_2 + \frac{\partial B_3}{\partial T}\dot{\beta}_3 + \frac{\partial Y}{\partial T}\dot{\gamma} + \frac{\partial Z}{\partial T}\dot{\mu}\right]. \qquad (47)\end{aligned}$$

3. Model Verification

In order to evaluate the model capability to describe the thermomechanical coupling of SMA, a numerical procedure developed by Savi et al. (2002) and Paiva et al. (2005) is employed to deal with the nonlinearities in the formulation. Basically, the procedure employs a operator split technique together with a iterative process, using a projection algorithm to treat the subdifferentials.

By using this numerical procedure, numerical simulations are carried out for different physical situations. At first, a verification of the model results are developed comparing numerical results with those obtained from experimental analysis presented by (Shaw & Kyriades, 1995). This experimental tests consider NiTi wires subjected to different loading hates at different temperatures. Identified parameters for this SMA specimen are presented in Table 1.

Numerical simulations are carried out considering two different models: coupled and uncoupled. The first one considers all energy equation thermomechanical terms. On the other hand, the uncoupled model neglects these terms and the temperature is prescribed. The model verification consider a tensile test at environmental temperature $T = 70°C$ and three different loading rates ($\dot{\varepsilon}$): $0.04s^{-1}$ (Figure 1), $0.004s^{-1}$ (Figure 2), $0.0004s^{-1}$ (Figure 3).

Figures 1-3 presents the stress-strain curves together with the temperature evolution. Notice that the thermomechanical coupling causes a temperature increase during austenite-martensite phase transformation and a temperature decrease during reverse transformation. This behavior affects the stress-strain curves that presents a hysteresis loop reduction for faster loading rates. It is noticeable that both coupled and uncoupled models are able to capture the SMA rate-dependence characteristics. As expected, the uncoupled model is not capable to capture the temperature variations since it is a driving variable.

At this point, the SMA specimen is subjected to different cyclic loadings considering different frequencies. Basically, 20 cycles are considered at a temperature $T = 80°C$. At first, the loading is applied at $0.3Hz$ (Figure 4). Under this conditions, the SMA presents temperature oscillations due to phase transformation. For this frequency, there is a proper balance with the convection and the stress-strain curves presents just a small variation from one cycle to another. By increasing the frequency to $1Hz$ (Figure 5), the system response is significantly altered by temperature variations. Notice that convection effect tends to decrease due to high frequency loadings.

A tensile-compressive is now in focus. The SMA specimen is at $T = 70°C$ subjected to a loading rate $\dot{\varepsilon} = 0.04s^{-1}$. Under this condition, temperature variations may induce a tensile-compressive asymmetry since temperature variations due to tensile behavior may change critical phase transformation stress level.

Table 1. Thermomechanical properties of the material.

Material Properties				
$E_A\,(Pa)$	$E_M\,(Pa)$	$\alpha^T\,(Pa)$	$\alpha^C\,(Pa)$	ε_R
67×10^9	25×10^9	120×10^6	120×10^6	74×10^4
$L_0^T\,(Pa)$	$L^T\,(Pa)$	$L_0^M\,(Pa)$	$L^M\,(Pa)$	$K_A\,(Pa)$
1×10^5	200×10^5	1×10^5	900×10^5	1.4×10^9
$K_M\,(Pa)$	$H_A(Pa)$	$H_M(Pa)$	$\Omega_A\,(Pa/K)$	$\Omega_M\,(Pa/K)$
0.4×10^9	4×10^9	1.1×10^9	0.74×10^6	0.17×10^6
$\eta_C^T\,(Pa.s)$	$\eta_D^T\,(Pa.s)$	$\eta_C^M\,(Pa.s)$	$\eta_D^M\,(Pa.s)$	$\rho\,(kg/m^3)$
10×10^5	45×10^5	10×10^5	45×10^5	6.45×10^3
$c\,(J/K)$	$T_A\,(K)$	$T_M\,(K)$	$T_0\,(K)$	$T_F\,(K)$
600	302	272	343	450

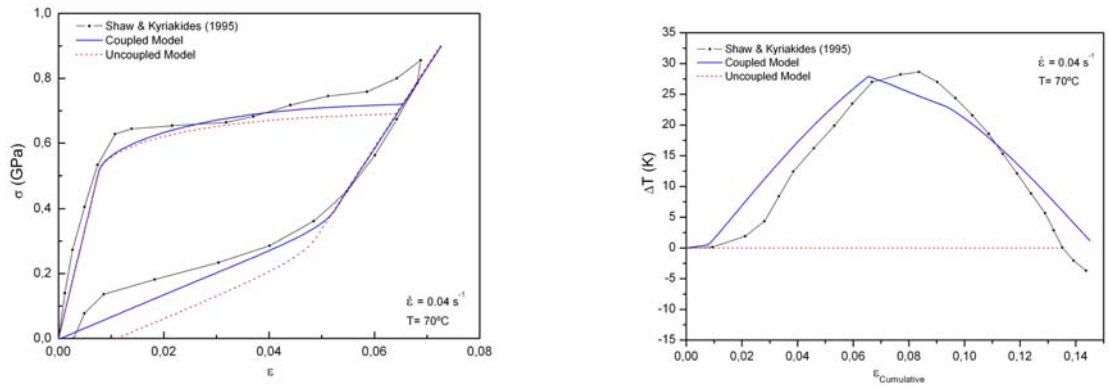

Figure 1. Comparative results between coupled and uncoupled model, stress-strain (left) and cumulative strain-temperature (right) with $\dot{\varepsilon} = 0.04s^{-1}$.

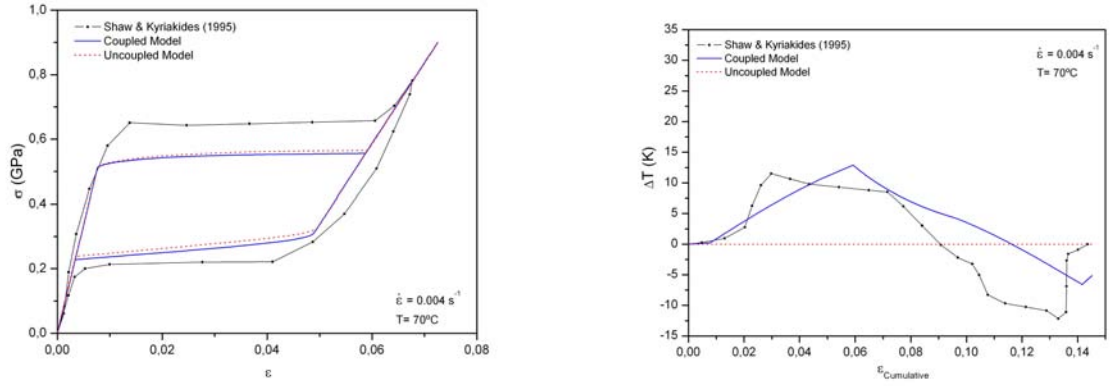

Figure 2. Comparative results between coupled and uncoupled model, stress-strain (left) and cumulative strain-temperature (right) with $\dot{\varepsilon} = 0.004s^{-1}$.

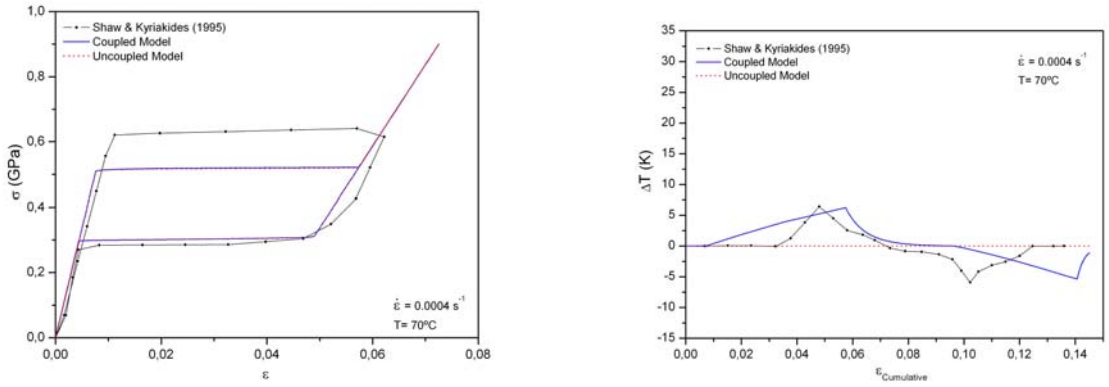

Figure 3. Comparative results between coupled and uncoupled model, stress-strain (left) and cumulative strain-temperature (right) with $\dot{\varepsilon} = 0.0004s^{-1}$.

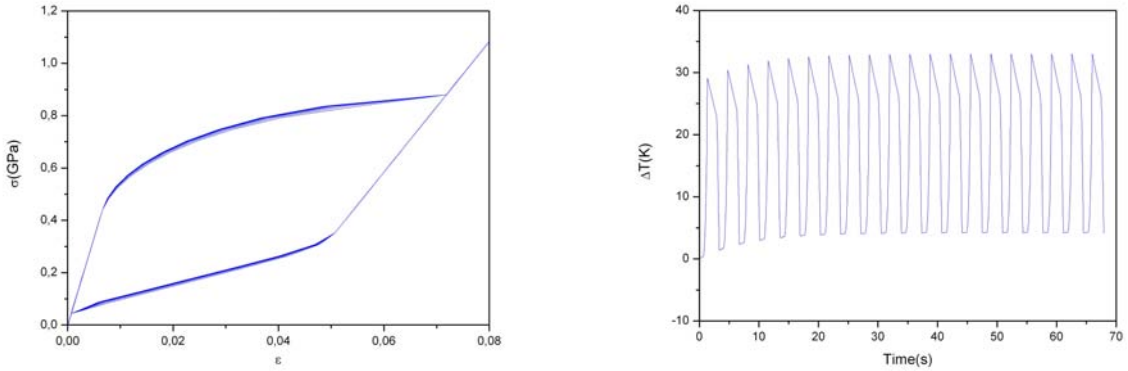

Figure 4. Cyclic load at $0.3Hz$, stress-strain (left) and temperature (right).

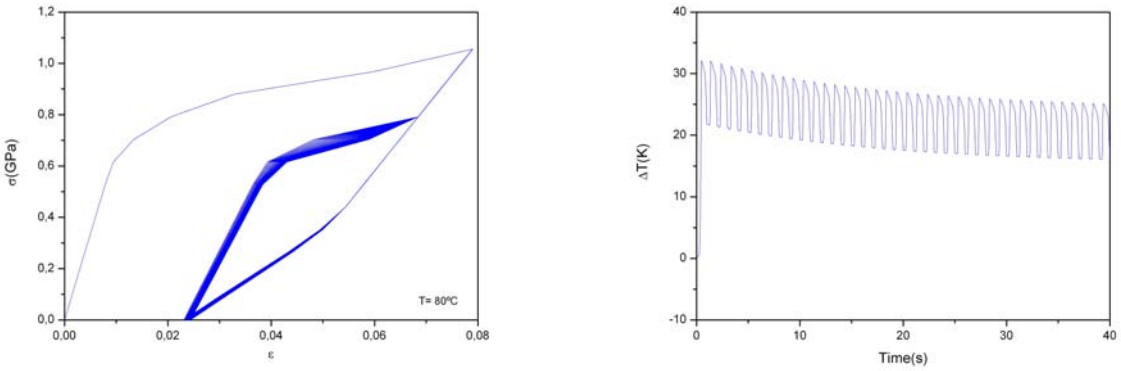

Figure 5. Cyclic load at $1Hz$, stress-strain (left) and temperature (right).

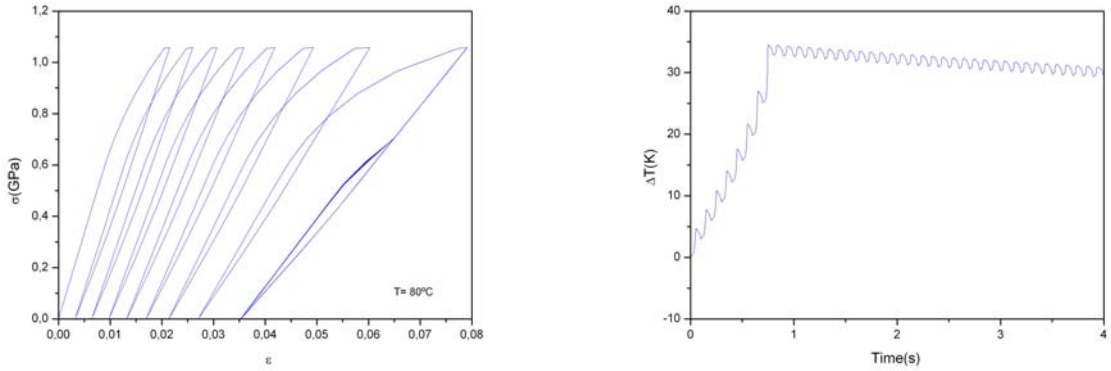

Figure 6. Cyclic load at $10Hz$, stress-strain (left) and temperature (right).

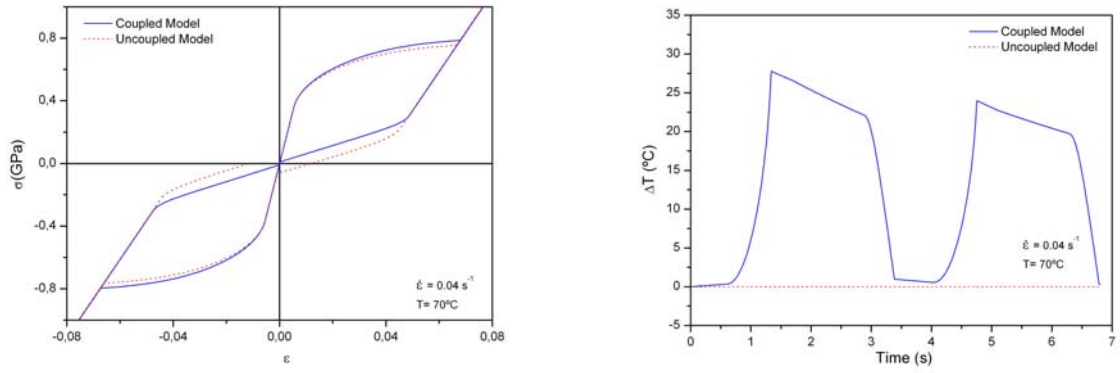

Figure 7. Comparative results between coupled and uncoupled model, stress-strain (left) and temperature variation(right) with $\dot{\varepsilon} = 0.04s^{-1}$.

4. CONCLUSIONS

This article discusses the phenomenological model to describe the shape memory alloy behavior considering thermo-mechanical coupling. The model is built upon a previous version developed by Paiva et al. (2005). The thermomechanical coupling is now in focus. Numerical simulations establish a comparison between numerical and experimental results showing a close agreement for different loading rates. This rate-dependence characteristics is captured by the uncoupled model as well, showing its capability to describe this kind of behavior.

5. ACKNOWLEDGEMENTS

The authors would like to acknowledge the support of CNPq and ANP.

6. REFERENCES

Bo, Z.H. and Lagoudas, D.C., (1999). "Thermomechanical modeling of polycrystalline SMAs under cyclic loading. Part III: evolution of plastic strains and two-way shape memory effect", International Journal of Engineering Science 37, no. 9, 1175-1203.

Paiva, A., Savi, M.A., (2006). "An Overview of Constitutive Models for Shape Memory Alloys", Mathematical Problems in Engineering, v.2006, Article ID56876, pp.1-30. ISSN 1024-123X.

Savi, M.A., Paiva, A., Baêta-Neves, A.P. and Pacheco, P.M.C.L.,(2002). "Phenomenological modeling and numerical simulation of shape memory alloys: a thermo-plastic-phase transformation coupled model" , Journal of Intelligent Material Systems and Structures 13 , no. 5, 261-273.

Baêta-Neves, A.P., Savi, M.A. and Pacheco, P.M.C.L., (2004). "On the Fremond's constitutive model for shape memory alloys", Mechanics Research Communications 31 , no. 6, 677-688.

Paiva, A., Savi, M.A., Braga, A.M.B. & Pacheco, P.M.C.L., (2005a), "A Constitutive Model for Shape Memory Alloys Considering Tensile-Compressive Asymmetry and Plasticity", International Journal of Solids and Structures, v.42, n.11-12, pp.3439-3457, ISSN 0020-7683.

Savi, M.A. and Paiva, A., (2005). "Describing internal subloops due to incomplete phase transformations in shape memory alloys", Archive of Applied Mechanics 74 , no. 9, 637-647.

Shaw, J.A., Kyriakides, S., (1995). "Thermomechanical Aspects of Ni-Ti", Journal of the Mechanics and Physics of Solids, Vol. **43**, n. 8, p. 1243.

Auricchio, F., Reali, A. and Stefanelli, U., (2007). "A three-dimensional model describing stress-induced solid phase transformation with permanent inelasticity" International Journal of Plasticity 23, 207-226.

Rockafellar, R.T.,(1970). Convex analysis, Princeton Press.

7. Responsibility notice

The author(s) is (are) the only responsible for the printed material included in this paper